How to cite: *Angew. Chem. Int. Ed.* **2024**, *63*, e202411554
doi.org/10.1002/anie.202411554

Endergonic Synthesis | Hot Paper

Progressive Endergonic Synthesis of Diels–Alder Adducts Driven by Chemical Energy

*Shaymaa Al Shehimy, Hai-Dang Le, Shuntaro Amano, Simone Di Noja, Luca Monari, and Giulio Ragazzon**

Abstract: The overwhelming majority of artificial chemical reaction networks respond to stimuli by relaxing towards an equilibrium state. The opposite response—moving away from equilibrium—can afford the endergonic synthesis of molecules, of which only rare examples have been reported. Here, we report six examples of Diels–Alder adducts formed in an endergonic process and use this strategy to realize their stepwise accumulation. Indeed, systems respond to repeated occurrences of the same stimulus by increasing the amount of adduct formed, with the final network distribution depending on the number of stimuli received. Our findings indicate how endergonic processes can contribute to the transition from responsive to adaptive systems.

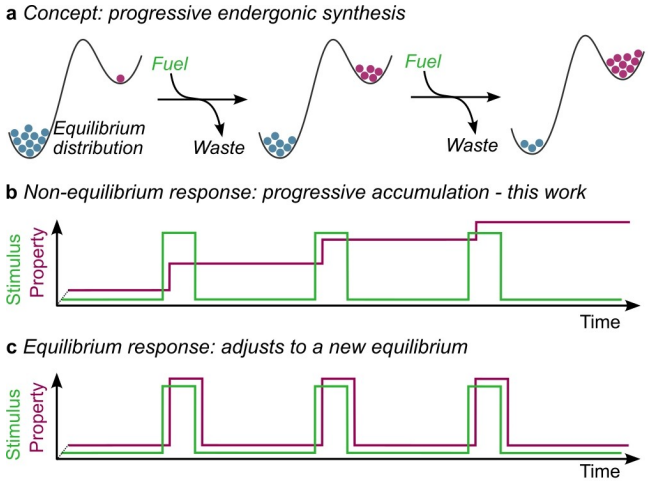

Figure 1. a) Concept of progressive endergonic synthesis: the repeated addition of a chemical fuel progressively shifts the reaction interconverting two species represented as blue and purple dots, to over-accumulate one of them, here the purple ones. b) Illustration of a non-equilibrium progressive accumulation of a given species in response to a transient stimulus. c) Classical switching response, governed by equilibrium thermodynamics.

Introduction

Molecular machines use energy to realize directional motion. The kinetic mechanisms allowing this energy to be fruitfully used—instead of just being dissipated into heat—are called molecular ratchet mechanisms.[1–5] In recent years, it has become clear that ratchet mechanisms can be used to promote a multitude of energy-demanding processes (having $\Delta G > 0$), which are technically termed *endergonic*.[3,5–7] For example, ratchet mechanisms can be designed to promote the accumulation of a certain species at concentrations not compatible with equilibrium,[8] a process referred to as endergonic synthesis.[7] It implies the presence of a "driving" reaction, which shifts the target "driven" reaction away from equilibrium thanks to the underlying ratchet mechanism (Figure 1a). The reagent of the driving reaction has often been identified as a chemical fuel, which is the definition we adopt herein.[9,10]

Besides molecular machines,[11–16] examples in this area are essentially limited to few deracemizations[17–19] and mostly individual cases of dynamic-covalent reactions.[7,20–24] Usually, such systems exploit a templating agent that is removed to afford a metastable distribution.[21–23] In a recent example of this type, a hydrazone with substrate-induced[25–27] catalytic properties could be over-accumulated (from 47 % to 83 %).[23] While preparing this manuscript, a preprint presented the formation of a Diels–Alder adduct (up to 15 %) with high regio- and stereoselectivity, by using carbodiimide to tether two reactants transiently.[24,28] Indeed, when catalyzed by acids, carbodiimide hydration results in the transient formation of covalent bonds,[29–31] and this phenomenon proved versatile to drive non-equilibrium processes, being fruitfully used in relation to both molecular machines, self-assembly, and reactivity modulation.[9,16,32–35] In contrast with the classical activation chemistry of carboxylic acids, in all these cases, the coupled process (e.g., conformation changes, assembly of monomers) is formally unrelated to acid activation.[6]

Mastering endergonic synthesis allows processes that are not possible using equilibrium chemistry. A significant example is the progressive[5] accumulation of a given high-

[*] S. Al Shehimy, H.-D. Le, S. Amano, S. Di Noja, L. Monari, G. Ragazzon
University of Strasbourg, CNRS, Institut de Science et d'Ingénierie Supramoléculaires (ISIS) UMR 7006
8 allée Gaspard Monge, 67000 Strasbourg, France
E-mail: ragazzon@unistra.fr

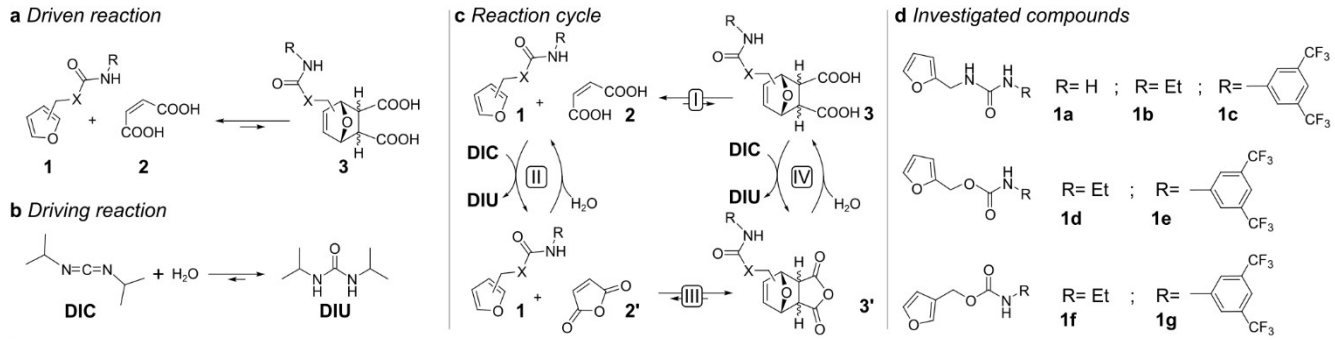

Figure 2. a) Driven reaction: the target reaction to be shifted away from equilibrium, with X and R specified for the investigated compounds in panel d. b) Driving reaction, providing energy to the system. c) Reaction cycle coupling the driven reaction **I** to the driving one—carbodiimide hydration—which can be catalyzed via either steps **II** or **IV**; the cycle is completed by reaction **III**, which is both kinetically and thermodynamically favored with respect to reaction **I**. The reaction network with explicit indication of *endo*- and *exo*-adducts is provided as Figure S1. d) Investigated compounds, in addition to 3-methylfuran (**1h**, see below).

energy species upon multiple temporary exposures to a chemical stimulus, as illustrated in Figure 1b. In contrast with equilibrium systems, the repeated exposure does not simply induce a switching process (Figure 1c) but results in the progressive accumulation of species. Such a behavior has been explicitly identified as a future challenge[36] in the context of adaptive materials.[36,37]

Here, we leverage endergonic synthesis driven by chemical catalysis to realize the progressive accumulation of small molecules. In particular, we use carbodiimide hydration to power the endergonic formation of multiple Diels–Alder adducts, producing the progressive response illustrated in Figure 1a,b upon repeated addition of a chemical fuel.

Results and Discussion

We focused our attention on the inefficient reaction of furan-based dienes of type **1** (Figure 2a), which barely react with maleic acid **2** to form adducts **3**. This is the reaction that we want to promote despite having a $\Delta G > 0$ under the employed conditions. As energy source, we employed the exergonic hydration reaction of *N*,*N*′-diisopropylcarbodiimide (**DIC**) to give the corresponding urea (**DIU**, Figure 2b). Indeed, activation of acid **2** with **DIC** affords maleic anhydride **2**′, which is a more activated dienophile towards Diels–Alder reactions, both kinetically and thermodynamically.[38] The resulting reaction network is shown in Figure 2c. The change in reaction properties between steps **I** and **III** may already install a ratchet effect under alternating conditions. Yet, hydrogen bond donors in **1** may also produce kinetic differences in **DIC** hydration and anhydride hydrolysis (steps **II** and **IV**) providing an additional information ratchet effect.[16,39] On this ground, a screening of several derivatives bearing hydrogen bond donors brought us to focus on dienes **1a**–**g**, having pendant urea or carbamate moieties (Figure 2d). These compounds are readily available upon reaction of the corresponding isocyanates with aminomethylfuran or hydroxymethylfuran (see Supporting Information sections 1–3 for synthetic details). 3-methylfuran (**1h**), lacking hydrogen bond donors, was used as a control compound.

After a screening of temperatures and solvents, we selected as operating conditions a temperature of 40 °C and the mixed solvent $CD_3CN:D_2O$ 85:15. Under these conditions, the half-life of maleic anhydride **2**′ is about 4 hours. This time scale should be compatible with reaction **III**; therefore, we tested the reaction of **2**′ with dienes **1a**–**h**. Mixing these compounds in CD_3CN at 100 mM affords new NMR peaks consistent with the formation of the corresponding Diels–Alder adducts. The identity of the new species was confirmed by bidimensional NMR, HPLC coupled to high-resolution mass spectrometry analysis, and computational modeling (see Supporting Information section 4). As the data in Table 1 indicates, the reaction proceeded in fair yields for most compounds in 48 h, with a marked preference for the formation of *exo*-**3**′ over *endo*-**3**′. The extent of reaction at 48 h was considered unsatisfactory only for compounds **1d** and **1e**, the carbamate derivatives of 2-hydroxymethylfuran, and these compounds were not further studied. In contrast, the best results were obtained with carbamates **1f** and **1g**, prepared from 3-hydroxymethylfuran. The higher conversion observed in 3-substituted derivatives vs 2-substituted ones (e.g., **1d** vs **1f**) is attributed primarily to steric factors, on the basis of previous studies.[38]

Table 1: Yields of the Diels–Alder reaction (**III**) between furan-based dienes **1** and anhydride **2**′, both 100 mM in CD_3CN at 40 °C, monitored at 48 h.

Diene	Yield[a] (% of *exo*-adduct)	*exo*:*endo*
1a	20	96:4
1b	20	96:4
1c	21	96:4
1d	7[b]	95:5
1e	5	96:4
1f	46	>99:1
1g	32	>99:1
1h	72	99:1

[a] NMR yields of the major adduct, obtained using an internal standard. [b] Data obtained at 42 h.

The same species observed in pure acetonitrile form also when mixing the starting materials in the target aqueous solvent, with the newly formed species disappearing after some time. The experimental observations are consistent with the hydrolysis of Diels–Alder adducts **3′** to give **3**, as the same species could also be detected (albeit just in traces in most cases) when equilibrating a mixture of **1** and **2** under the same conditions (SI section 4c, Figures S73 and S74). For example, mixing 100 mM of **1f** and **2′** in the aqueous mixed solvent afforded *exo*-**3f′**, with its concentration peaking at ca. 15 mM after 7 h, to then hydrolyze to *exo*-**3f** (Figure S74). Importantly, *exo*-**3f** accumulated in concentration far from equilibrium slowly reverted towards its thermodynamic equilibrium with **1f** and **2** (as observed in other experiments, see below), confirming that reaction **I** is not thermodynamically favored.

These preliminary studies indicated which of the selected compounds have suitable thermodynamic and kinetic properties for reactions **I** and **III**. The outlined premises are sufficient to approach the endergonic formation of adducts *exo*-**3**, i.e., their synthesis in conditions when they are not thermodynamically stable.[7] To this aim, we pre-equilibrate mixtures of **1a–c**,**f–h** and **2**, and then add three equivalents of **DIC**. In all cases we could observe the counterclockwise sequence of reactions **II**→**III**→**IV** shown in Figure 1c: first anhydride **2′** formed, followed by adduct *exo*-**3′**, which then hydrolyzed to give *exo*-**3**. We can use the reactivity of **1f** as a representative example to give a blueprint of the timescales involved in the counterclockwise cycle: the half-life of **II** is <2 min, **III** and **IV** have longer half-lives of 19 h and 16 h respectively (Figure S55, S83a). The half-life of the retro Diels Alder **I** is 29 h (Figure S58), making it the slowest step of the cycle, which favors the accumulation of **3f** away from equilibrium. To compare a non-equilibrium state with the corresponding equilibrium we considered the moment in time when anhydrides **2′** and **3′** had completely hydrolyzed (usually ≤ 1 % residue). The results are reported in Figure 3a and Supporting Information section 5d. In all cases the successful endergonic synthesis of Diels–Alder adducts was achieved, with yields ranging from 3 to 28 %.

The non-equilibrium nature of the observed phenomena was further confirmed by the fact that mixtures slowly evolved towards the initial equilibrium distribution. Control experiments excluded a role of accumulation of **DIU** in promoting the observed accumulation of adducts **3**; in fact, its presence shifts the equilibrium distribution of reaction **I** even slightly more towards the separated components (Table S1). Interestingly, for all the 2-substituted derivatives (**1a–c**) the *endo*-/*exo*- selectivity was inverted. For example, **1a** formed preferentially the *endo*-adduct under thermodynamic control, while the *exo*-adduct was majorly detected under non-equilibrium conditions. On the other hand, 3-substituted furans afford the best selectivity, with *exo*-**3f** and *exo*-**3g** being the sole detected isomers. These observations corroborate the idea that endergonic synthesis can be used to control selectivity.[24] We used density functional theory

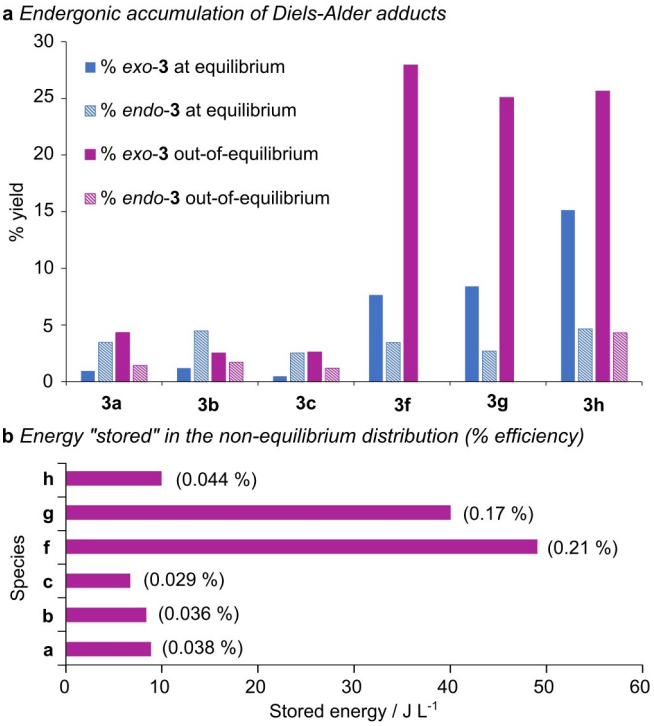

Figure 3. a) Comparison between the % yield of Diels–Alder adducts **3** at equilibrium (blue bars) and away from equilibrium (purple bars), the latter obtained upon adding 3.0 equivalents of **DIC** to an equilibrated mixture of **1** and **2** and allowing subsequent hydrolysis of formed anhydrides **3′**. Full and striped bars refer to *exo*- and *endo*- adducts, respectively. No *endo*- adduct is observed for **3f** and **3g**. b) Calculated stored energy for non-equilibrium distribution in panel a, with the corresponding % efficiencies shown in parentheses. Conditions: $CD_3CN:D_2O$ 85:15 at 40 °C; 100 mM of both **1** and **2**.

(DFT) calculations to shed light on the origin of selectivity inversion. Comparing the most stable adduct structures for **1a**, **1d**, and **1f** revealed that only in 2-substituted *endo*-adducts with acid **2** the acid moiety forms a hydrogen bond with the carbonyl oxygen, stabilizing the *endo*-adduct structure thermodynamically (see Supporting Information section 9). This interaction is absent in 3-substituted derivatives and cannot be formed when anhydride **2′** reacts. Indeed, the fueled pathway displays the typical *exo*-selectivity of maleic anhydride with furans, explaining the observed selectivity inversion.[38]

Based on the population of **1**, **2**, *endo*-**3**, and *exo*-**3** species at equilibrium and upon fueling, we calculated the energy stored in the non-equilibrium distributions (Figure 3b, see Supporting Information section 8 for details). Dividing the stored energies by the energy supplied by the driving hydration reaction, we also calculated the corresponding thermodynamic efficiencies (Figure 3b, values in parenthesis).[6,40,41] Among the six species investigated, **f** and **g** showed the highest stored energy, reaching 49 and 40 J/L, respectively. Comparing these values with other chemically-fueled systems, we observe that the present ones are comparatively high among chemically driven systems. Previous reports of stored energy range from

0.49 J/L in the adenosine triphosphate-driven formation of a catalytic hydrazone,[23] to 3.0–4.4 J/L in a range of interlocked structures,[42,43] and 14 J/L in a Diels–Alder adduct (see Supporting Information section 8).[24] The amount of stored energy is even comparable with the one estimated for a polymer chain entanglement produced by a light-driven molecular rotor, greater than 72 J/L (see Supporting Information section 8).[44] One of the reasons for the high energies stored in the present case is that the employed concentrations are also higher (high vs low mM). Yet, operating at a higher concentration does not merely scale linearly the stored energy, since higher concentrations favor the second-order Diels–Alder reaction **III**. We confirmed the non-linearity by repeating the fueling of **3f** at 25 mM instead of 100 mM (Figure S80). When the concentration is four times lower, the stored energy drops from 49 J/L to 5 J/L (Table S6), decreasing by one order of magnitude.

Having established the endergonic formation of a family of Diels–Alder adducts, we attempted the realization of a multistep non-equilibrium process. To this aim, we focused on the best-performing dienes, **1f** and **1g**. In the key experiment, the addition of **DIC** is repeated before the system returns to equilibrium, yet after anhydrides **2**′ and **3**′ have hydrolyzed. When performing this experiment with **1f**, by adding 1.6 equivalents of **DIC** twice, the amount of adduct *exo*-**3f** increases from its equilibrium value of 7 % to 24 % after the first addition, further increasing to 27 % after the second one, before evolving towards the equilibrium distribution (Figure 4a and S76). An analogous behavior is observed with compound **1g**, for which the amount of adduct *exo*-**3g** increases from 7% at equilibrium to 18 to 24 % when subject to the same sequence of additions (Figure 4b). The reproducibility of multistep responses was confirmed by repeating the experiments either two (**1f**) or three (**1g**) times, obtaining an error of ±1.3 % on the final plateau in the case of **1g** (Figure S77, S78).

Performing the same type of experiment but adding 1.0 equivalent three times affords a multistep response. For example, in the case of **1f**, the amounts of *exo*-**3f** accumulated are 18, 23, and 24 % compared to 10 % at equilibrium (Figure 4c, lighter bars and S79a). Fueling **1g** three times affords a similar profile response, with 23 % of **3g** accumulated upon the third cycle (Figure 4c, darker bars and S79b). Such multistep profiles are qualitatively analogous to those of synthetic polymers able to undergo irreversible mechanochemical strengthening upon cross-linking, a training behavior.[45,46] However, the endergonic essence of progressive accumulation enables reversibility, as the reaction network returns to equilibrium.

The progressive increase in the concentration of *exo*-**3f** and *exo*-**3g** observed in multi-cycle experiments also corresponds to an increase in the stored energy. The values of stored energy and corresponding thermodynamic efficiencies were calculated for all multi-cycle experiments (Figure 4d and Supporting Information section 8). Using as an example the 3-step experiment performed with **1f**, after addition of 1.0 equivalent of **DIC** for three times, the stored

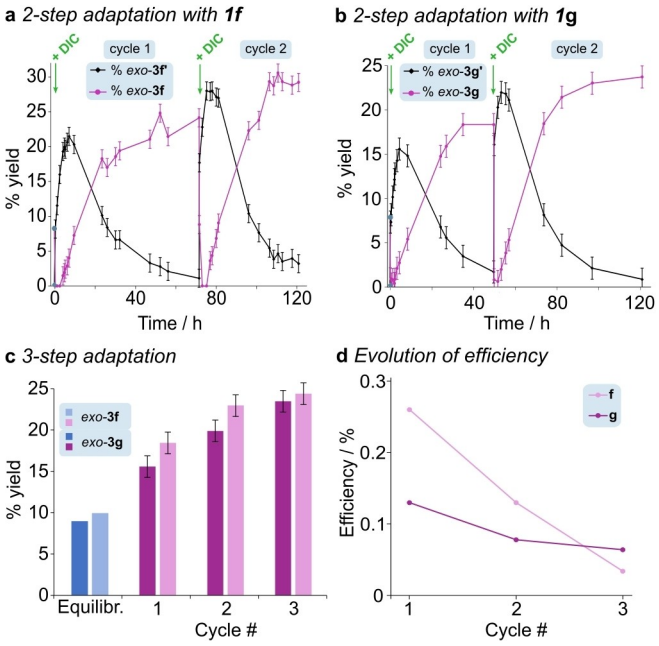

Figure 4. Evolution in time of the % yield of a) *exo*-**3f** (purple) and *exo*-**3f**′ (black) or b) *exo*-**3g** (purple) and *exo*-**3g**′ (black) adducts, upon repeated additions of 1.6 or 1.5 equivalents of **DIC**, respectively, performed in correspondence of the arrows. The experiment starts from the equilibrium distribution of **1f** or **1g**, **2**, and **3f** or **3g** (blue circle/diamond at t = 0), with concentrations monitored by ^{1}H NMR. c) % yield of *exo*-**3f** (pale-colored bars) and *exo*-**3g** (deep-colored bars), obtained upon repeated additions of 1.0 equivalent of **DIC**. d) Evolution of efficiency of energy storage with respect to **f** (pale purple line) and **g** (deep purple line), upon repeated additions of 1.0 equivalent of **DIC**. Conditions: $CD_3CN:D_2O$ 85:15 at 40 °C, 100 mM of both **1f** or **1g** and **2**. Error bars refer to the standard deviation of ±1.3 % yield measured for the endpoint of the fueling experiment in panel b, which was taken as reference (see Supporting Information section 5b).

energy increases by 21, 9.5, and 2.5 J/L. This observation means that the efficiency of the energy storage process decreases with subsequent fueling cycles, going from 0.26 % in the first cycle to 0.034 % in the third one (Figure 4d). A similar behavior was observed with compound **1g**. Upon adding 1.0 equivalent of **DIC** three times, the overall stored energy increased, while the efficiency dropped, albeit less abruptly, from 0.13 % to 0.064 % (Figure 4d). Still focusing on **1f**, we attempted pushing the number of sequential steps to the limit by adding 1.5 equivalents of **DIC** several times, and we reached a plateau after 4 steps (Figure S81). This limit is likely not due to waste accumulation: a control fueling experiment in the presence of purposely added waste (Figure S82) produced profiles comparable with those of experiments done in its absence. Indeed, in contrast with typical non-equilibrium refueling experiments—where the same process is repeated—here each fuel addition promotes an additional step that brings the system further away from equilibrium.

Multiple effects contribute to the observed multistep response. A key design element is that reactions **II** and **IV** (anhydride formation and hydrolysis) are faster than reaction **III**, with reaction **I** being the slowest. As a result, when

anhydrides have hydrolyzed, reaction **III** has not reached equilibrium yet, and pulses of **DIC** can lead to different outcomes, depending on the initial conditions. This behavior differs from the classical description of energy ratchet effects, where equilibration of reaction **III** is typically assumed. Information ratchet effects rely on differences in the rates of reaction **II** and **IV**, leading to kinetic asymmetry (see Supporting Information section 5a for a discussion on the relation with existing theoretical frameworks).[47] Here, the progressive response could be favored by a faster hydrolysis of **3′** to **3**, compared to the hydrolysis of **2′** to **2**, possibly promoted by the carbamate group introduced in the investigated compounds.

To gain insights on this effect, we attempted the multi-step experiment adding three times one equivalent of **DIC** to control compound **1h**, which is an analog of **1f** lacking any hydrogen bond donor in its structure. The product of the endergonic process, *exo*-**3h**, reached 24 % after the addition of 1.0 equivalent of **DIC** (vs 16 % under equilibrium conditions), yet a similar amount of *exo*-**3h** was observed also in subsequent cycles (Figure 5a). The lack of a progressive accumulation may be due to the fact that the half-life of anhydride *exo*-**3h′** (20 h in the presence of 3 equivalents of **DIC**) is longer than that of anhydrides *exo*-**3f′** and *exo*-**3g′** (ca. 16 h) and remains unchanged if an external carbamate is also added (Figure 5b), indicating that the enhanced hydrolysis observed in *exo*-**3f′** and *exo*-**3g′** is due to an apparently intramolecular effect.

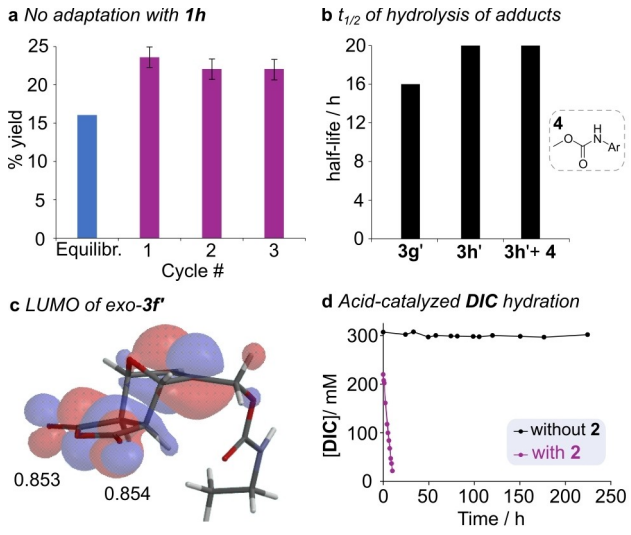

Figure 5. a) % yield of *exo*-**3h** obtained upon repeated additions of 1.0 equivalent of **DIC** under the same conditions used in Figure 4. b) half-life of anhydride adducts **3g′**, **3h′**, and **3h′** in the presence of 1.0 equivalent of carbamate **4**; c) LUMO of *exo*-**3f′** in its minimum energy structure, with indication of the atomic charges at the carbonyl carbon atoms. d) Evolution in time of [**DIC**] in the presence (purple) or absence (black) of **1f** and **2**. The former is extracted from the fueling experiment of **1f**+**2**↔**3f** with 3 equivalents of **DIC** in $CD_3CN:D_2O$ (85:15), 40 °C Error bars in panel a refer to the standard deviation of ±1.3 % yield measured for the endpoint of the fueling experiment in Figure 4b.

To evaluate the role of electronic effects we calculated the atomic charges at the carbonyl carbon atoms in *exo*-**3f′** and *exo*-**3h′**. DFT calculations confirmed that the lowest unoccupied molecular orbital (LUMO) is centered at the carbonyl groups, however the atomic charges at the relevant carbon atoms do not differ significantly in *exo*-**3f′** and *exo*-**3h′**, being always close to 0.853 (Figure 5c and S88). In *exo*-**3f′** the distance between the carbamate oxygen and the nearest anhydride carbonyl is 4.52 Å, which might be bridged by a network of few water molecules. It is known that water clusters including up to seven molecules form in similar $CH_3CN:H_2O$ mixtures.[48] This phenomenon could play a role here, however its investigation goes beyond the scope of the present work, being the subject of dedicated studies.

Overall, these experiments suggest that introducing a carbamate group leads to a sufficient kinetic asymmetry. Clearly, in the presented systems the carbamate group is necessary to observe a progressive response. Moreover, to confirm that the partner of the Diels–Alder reaction catalyzes **DIC** hydration, we monitored the stability of **DIC** over time in the absence or absence of **1f** and **2** (Figure 5d). In their absence, no significant conversion to **DIU** was observed over at least 220 h, while in sharp contrast the half-life of **DIC** drops to 2.8 h in their presence, confirming the occurrence of catalysis.

Conclusions

We have shown that a family of Diels–Alder adducts can be formed under thermodynamically unfavored conditions, powered by the catalysis of carbodiimide hydration. The endergonic reactions take place with yields up to 28 %, and diastereoselectivity up to 99:1. We leveraged endergonic reactions to realize non-equilibrium adaptation processes, focusing on the progressive accumulation of target species. The observed behavior maps a characteristic of the Venus flytrap, where an increasing amount of electrical charge is accumulated after each touch, in the case of the carnivorous plant, leading to closure once a threshold is reached.[49] Both here and in flytraps, if a sufficient amount of time is given the system returns to equilibrium, losing the memory of past events. This aspect further differentiates the present systems from the carbodiimide-promoted formation of amide bonds in water, which are practically irreversible. Overall, this study provides concrete examples of how endergonic processes can contribute to the transition from responsive to adaptive systems.

Supporting Information

We cited additional references within the SI.[50–54]

Acknowledgements

This work was supported by the Interdisciplinary Thematic Institute ITI-CSC via the IdEx Unistra (ANR-10-IDEX-0002) within the program Investissement d'Avenir and the European Research Council (ERC-2021-StG n. 101041933). H.L. and L.M. thank the CSC Graduate School funded by the French National Research Agency (CSC-IGS ANR-17-EURE-0016) for a MSc fellowship. The authors thank Cyril Antheaume, Dr. Claudia Bonfio, Ahmad Bachir, Thitiporn Sangchai, and Bharath Vinjamuri for their help in preliminary experiments and analytical measurements.

Conflict of Interest

The authors declare no conflict of interest.

Data Availability Statement

The data that support the findings of this study are available in the supplementary material of this article.

Keywords: non-equilibrium systems · endergonic processes · systems chemistry · dynamic covalent chemistry · catalysis

[1] R. D. Astumian, *Phys. Chem. Chem. Phys.* **2007**, *9*, 5067–83.
[2] P. M. Hoffmann, *Life's Ratchet. How Molecular Machines Extract Order from Chaos*, Basic Books, New York, **2012**.
[3] E. R. Kay, D. A. Leigh, F. Zerbetto, *Angew. Chem. Int. Ed.* **2007**, *46*, 72–191.
[4] M. Baroncini, S. Silvi, A. Credi, *Chem. Rev.* **2020**, *120*, 200–268.
[5] S. Borsley, B. M. W. Roberts, D. A. Leigh, *Angew. Chem. Int. Ed.* **2024**, e202400495.
[6] T. Sangchai, S. Al Shehimy, E. Penocchio, G. Ragazzon, *Angew. Chem. Int. Ed.* **2023**, e202309501.
[7] S. Borsley, J. M. Gallagher, D. A. Leigh, B. M. W. Roberts, *Nat. Chem. Rev.* **2023**, 8–29 .
[8] G. Ragazzon, L. J. Prins, *Nat. Nanotechnol.* **2018**, *13*, 882–889.
[9] S. Borsley, D. A. Leigh, B. M. W. Roberts, *Nat. Chem.* **2022**, *14*, 728–738.
[10] I. Aprahamian, S. M. Goldup, *J. Am. Chem. Soc.* **2023**, *145*, 14169–14183.
[11] M. Von Delius, E. M. Geertsema, D. A. Leigh, D. T. D. Tang, *J. Am. Chem. Soc.* **2010**, *132*, 16134–16145.
[12] C. Cheng, P. R. McGonigal, W. G. Liu, H. Li, N. A. Vermeulen, C. Ke, M. Frasconi, C. L. Stern, W. A. Goddard, J. F. Stoddart, *J. Am. Chem. Soc.* **2014**, *136*, 14702–14705.
[13] S. Erbas-Cakmak, S. D. P. Fielden, U. Karaca, D. A. Leigh, C. T. McTernan, D. J. Tetlow, M. R. Wilson, *Science* **2017**, *358*, 340–343.
[14] Y. Qiu, B. Song, C. Pezzato, D. Shen, W. Liu, L. Zhang, Y. Feng, Q. H. Guo, K. Cai, W. Li, H. Chen, M. T. Nguyen, Y. Shi, C. Cheng, R. D. Astumian, X. Li, J. F. Stoddart, *Science* **2020**, *368*, 1247–1253.
[15] S. Amano, S. D. P. Fielden, D. A. Leigh, *Nature* **2021**, *594*, 529–534.
[16] S. Borsley, D. A. Leigh, B. M. W. Roberts, *J. Am. Chem. Soc.* **2021**, *143*, 4414–4420.
[17] A. D. Lackner, A. V. Samant, F. D. Toste, *J. Am. Chem. Soc.* **2013**, *135*, 14090–14093.
[18] Y. Ji, L. Shi, M. W. Chen, G. S. Feng, Y. G. Zhou, *J. Am. Chem. Soc.* **2015**, *137*, 10496–10499.
[19] S. Borsley, E. Kreidt, D. A. Leigh, B. M. W. Roberts, *Nature* **2022**, *604*, 80–85.
[20] H. Fanlo-Virgós, A.-N. R. Alba, S. Hamieh, M. Colomb-Delsuc, S. Otto, *Angew. Chem. Int. Ed.* **2014**, *53*, 11346–11350.
[21] L. Ratjen, G. Vantomme, J. M. Lehn, *Chem. Eur. J.* **2015**, *21*, 10070–10081.
[22] J. Holub, G. Vantomme, J. M. Lehn, *J. Am. Chem. Soc.* **2016**, *138*, 11783–11791.
[23] T. Marchetti, L. Gabrielli, D. Frezzato, L. J. Prins, *Angew. Chem. Int. Ed.* **2023**, e202307530.
[24] E. Olivieri, J. M. Gallagher, A. Betts, T. W. Mrad, D. A. Leigh, *ChemRxiv.* **2023**, DOI: 10.26434/chemrxiv-2023-6nqn3-v2.
[25] P. Solís Muñana, G. Ragazzon, J. Dupont, C. Z. J. Ren, L. J. Prins, J. L. Y. Chen, *Angew. Chem. Int. Ed.* **2018**, *57*, 16469–16474.
[26] S. Bal, K. Das, S. Ahmed, D. Das, *Angew. Chem. Int. Ed.* **2019**, *58*, 244–247.
[27] S. P. Afrose, C. Ghosh, D. Das, *Chem. Sci.* **2021**, *12*, 14674–14685.
[28] E. Olivieri, J. M. Gallagher, A. Betts, T. W. Mrad, D. A. Leigh, *Nat. Synth.* **2024**, 707–714.
[29] M. Tena-Solsona, B. Rieß, R. K. Grötsch, F. C. Löhrer, C. Wanzke, B. Käsdorf, A. R. Bausch, P. Müller-Buschbaum, O. Lieleg, J. Boekhoven, *Nat. Commun.* **2017**, *8*, 15895.
[30] L. S. Kariyawasam, C. S. Hartley, *J. Am. Chem. Soc.* **2017**, *139*, 11949–11955.
[31] L. S. Kariyawasam, M. M. Hossain, C. S. Hartley, *Angew. Chem. Int. Ed.* **2021**, *60*, 12648–12658.
[32] M. A. Würbser, P. S. Schwarz, J. Heckel, A. M. Bergmann, A. Walther, J. Boekhoven, *ChemSystemsChem* **2021**, *3*, e2100015.
[33] C. M. E. Kriebisch, A. M. Bergmann, J. Boekhoven, *J. Am. Chem. Soc.* **2021**, *143*, 7719–7725.
[34] F. Schnitter, B. Rieß, C. Jandl, J. Boekhoven, *Nat. Commun.* **2022**, *13*, 2816.
[35] A. M. Bergmann, J. Bauermann, G. Bartolucci, C. Donau, M. Stasi, A. L. Holtmannspötter, F. Jülicher, C. A. Weber, J. Boekhoven, *Nat. Commun.* **2023**, *14*, 6552.
[36] A. Walther, *Adv. Mater.* **2019**, 1905111.
[37] C. Kaspar, B. J. Ravoo, W. G. van der Wiel, S. V. Wegner, W. H. P. Pernice, *Nature* **2021**, *594*, 345–355.
[38] R. C. Cioc, M. Crockatt, J. C. van der Waal, P. C. A. Bruijnincx, *Angew. Chem. Int. Ed.* **2022**, *61*, e202114720.
[39] S. Borsley, D. A. Leigh, B. M. W. Roberts, I. J. Vitorica-Yrezabal, *J. Am. Chem. Soc.* **2022**, *144*, 17241–17248.
[40] E. Penocchio, R. Rao, M. Esposito, *Nat. Commun.* **2019**, *10*, 3865.
[41] S. Corrà, M. T. Bakić, J. Groppi, M. Baroncini, S. Silvi, E. Penocchio, M. Esposito, A. Credi, *Nat. Nanotechnol.* **2022**, *17*, 746–751.
[42] L. Binks, S. Borsley, T. R. Gingrich, D. A. Leigh, E. Penocchio, B. M. W. Roberts, *Chem* **2023**, *9*, 2902–2917.
[43] S. Di Noja, M. Garrido, L. Gualandi, G. Ragazzon, *Chem. Eur. J.* **2023**, *29*, e202300295.
[44] C. Gao, A. Vargas Jentzsch, E. Moulin, N. Giuseppone, *J. Am. Chem. Soc.* **2022**, *144*, 9845–9852.
[45] A. L. B. Ramirez, Z. S. Kean, J. A. Orlicki, M. Champhekar, S. M. Elsakr, W. E. Krause, S. L. Craig, *Nat. Chem.* **2013**, *5*, 757–761.
[46] T. Matsuda, R. Kawakami, R. Namba, T. Nakajima, J. P. Gong, *Science* **2019**, *363*, 504–508.
[47] B. A. K. Kriebisch, A. Jussupow, A. M. Bergmann, F. Kohler, H. Dietz, V. R. I. Kaila, J. Boekhoven, *J. Am. Chem. Soc.* **2020**, *142*, 20837–20844.

[48] J. Chen, P. H. L. Sit, *Chem. Phys.* **2015**, *457*, 87–97.
[49] A. G. Volkov, T. Adesina, V. S. Markin, E. Jovanov, *Plant Physiol.* **2008**, *146*, 694–702.
[50] R. G. Fischer, J. E. Lancaster, A. Zweig, *J. Org. Chem.* **1980**, *45*, 3597–3603.
[51] R. Rao, M. Esposito, *Phys. Rev. X* **2016**, *6*, 041064.
[52] S. Amano, M. Esposito, E. Kreidt, D. A. Leigh, E. Penocchio, B. M. W. Roberts, *Nat. Chem.* **2022**, *14*, 530–537.
[53] F. Tordini, A. Bencini, M. Bruschi, L. De Gioia, G. Zampella, P. Fantucci, *J. Phys. Chem. A* **2003**, *107*, 1188–1196.
[54] T. T. Truong, H. T. Nguyen, M. N. Phan, L. T. T. Nguyen, *J. Polym. Sci. Part A* **2018**, *56*, 1806–1814.

Manuscript received: June 19, 2024
Accepted manuscript online: July 17, 2024
Version of record online: September 12, 2024